

Article

Evaluating the Use of DMSP/OLS Nighttime Light Imagery in Predicting PM_{2.5} Concentrations in the Northeastern United States

Xueke Li ¹, Chuanrong Zhang ^{1,*}, Weidong Li ¹ and Kai Liu ²

¹ Department of Geography, University of Connecticut, Storrs, CT 06269, USA; xueke.li@uconn.edu (X.L.); weidong.li@uconn.edu (W.L.)

² Key Laboratory of Water Cycle & Related Land Surface Processes, Institute of Geographic Sciences and Natural Resources, Chinese Academy of Sciences, Beijing 100101, China; liukai_cas@yahoo.com

* Correspondence: chuanrong.zhang@uconn.edu

Academic Editors: Bailang Yu, Yuyu Zhou, Chunyang He, Xiaofeng Li and Prasad S. Thenkabail

Received: 3 May 2017; Accepted: 13 June 2017; Published: 16 June 2017

Abstract: Degraded air quality by PM_{2.5} can cause various health problems. Satellite observations provide abundant data for monitoring PM_{2.5} pollution. While satellite-derived products, such as aerosol optical depth (AOD) and normalized difference vegetation index (NDVI), have been widely used in estimating PM_{2.5} concentration, little research was focused on the use of remotely sensed nighttime light (NTL) imagery. This study evaluated the merits of using NTL satellite images in predicting ground-level PM_{2.5} at a regional scale. Geographically weighted regression (GWR) was employed to estimate the PM_{2.5} concentration and analyze its relationships with AOD, meteorological variables, and NTL data across the New England region. Observed data in 2013 were used to test the constructed GWR models for PM_{2.5} prediction. The Vegetation Adjusted NTL Urban Index (VANUI), which incorporates Moderate Resolution Imaging Spectroradiometer (MODIS) NDVI into NTL to overcome the defects of NTL data, was used as a predictor variable for final PM_{2.5} prediction. Results showed that Defense Meteorological Satellite Program/Operational Linescan System (DMSP/OLS) NTL imagery could be an important dataset for more accurately estimating PM_{2.5} exposure, especially in urbanized and densely populated areas. VANUI data could obviously improve the performance of GWR for the warm season (GWR model with VANUI performed 17% better than GWR model without NDVI and NTL data and 7.26% better than GWR model without NTL data in terms of RMSE), while its improvements were less obvious for the cold season (GWR model with VANUI performed 3.6% better than the GWR model without NDVI and NTL data and 1.83% better than the GWR model without NTL data in terms of RMSE). Moreover, the spatial distribution of the estimated PM_{2.5} levels clearly revealed patterns consistent with those densely populated areas and high traffic areas, implying a close and positive correlation between VANUI and PM_{2.5} concentration. In general, the DMSP/OLS NTL satellite imagery is promising for providing additional information for PM_{2.5} monitoring and prediction.

Keywords: PM_{2.5}; nighttime light (NTL); Vegetation Adjusted NTL Urban Index (VANUI); aerosol optical depth (AOD); geographically weighted regression (GWR)

1. Introduction

Fine particulate matter (known as PM_{2.5}, with an aerodynamic diameter less than 2.5 μm) is hazardous to human health [1,2]. Evidence from both long-term and short-term studies of PM_{2.5} suggests that high levels of PM_{2.5} can cause high rates of mortality [3,4], contribute to high risks of cardiovascular diseases [5,6], and lead to increased possibility of lung function decline [7,8]. Thus,

accurately characterizing the spatiotemporal distribution and variation in $PM_{2.5}$ concentration is crucial for laying a sound basis for improving public health.

In general, two approaches have been introduced to characterize surface $PM_{2.5}$ concentration. The first one is to use ground-based $PM_{2.5}$ monitoring networks. It can provide accurate measurements. However, its spatial coverage is limited and observed data are only available at certain times due to sampling frequencies. In addition, these point measurements are insufficient to explain regional variations, and thus are inevitably subject to errors when estimating $PM_{2.5}$ concentration at a regional scale [9]. By contrast, remote sensing (RS) technology can provide continuous spatial and temporal observations, which may help to solve the problem faced by monitoring networks. The RS approach uses satellite-retrieved aerosol optical depth (AOD) to estimate $PM_{2.5}$ pollution in areas where ground-based monitors are too sparsely distributed [10–12]. A growing body of work has been done on examining the relationship between RS-retrieved AOD from various sensors and ground-measured $PM_{2.5}$ [13–16]. Among them, Moderate Resolution Imaging Spectroradiometer (MODIS) imagery has been demonstrated to be a quality-guaranteed product and has been widely used in predicting $PM_{2.5}$ concentration [17,18]. Apart from AOD retrievals, meteorological variables and land use information, for instance, have also been utilized to develop more sophisticated statistical models for $PM_{2.5}$ estimation [14,19–25]. Results from these studies revealed that the incorporation of meteorological parameters and land use information into the $PM_{2.5}$ -AOD relationship can improve the performance of prediction models.

In the last two decades, the nighttime light (NTL) imagery from the Defense Meteorological Satellite Program/Operational Linescan System (DMSP/OLS) began to play an important role in various studies, including but not limited to detecting human settlements [26], estimating population density [27], and mapping urban extent [28–30]. Despite its wide use in demographic and socioeconomic studies, NTL data has received less attention in $PM_{2.5}$ pollution monitoring, especially in those studies concerning complex regions with both urban and rural settings. Only recently, a couple of studies investigated the effectiveness of DMSP/OLS NTL data in predicting daily $PM_{2.5}$ average concentration [31,32]. However, the DMSP/OLS NTL data were used as the only input variable in these studies for $PM_{2.5}$ prediction, and the potential contributions of meteorological variables and AOD measurements were ignored.

This study aimed to evaluate the potential of using DMSP/OLS NTL data, together with satellite-retrieved AOD data and meteorological data, to estimate the ground-level $PM_{2.5}$ concentration. The study area is the New England region, which is composed of urban, suburban, and rural areas. For this purpose, the geographically weighted regression (GWR) method [33] was chosen for performing $PM_{2.5}$ prediction. The performance of the specifically constructed GWR models with different input variables was cross-validated, and the spatiotemporal variability of the predicted $PM_{2.5}$ was demonstrated for the year 2013.

2. Materials and Methods

2.1. Study Area

Our study area is the New England region, Northeastern United States. It comprises the states of Maine (ME), New Hampshire (NH), Vermont (VT), Massachusetts (MA), Connecticut (CT), and Rhode Island (RI) (Figure 1). The entire New England region has an area of approximately 186,460 km², with a population of 14,444,865 as recorded in 2010. Among the six states, MA is the most populous while VT is the least populous. A prominent characteristic of New England is its densely distributed forests [34], which cover approximately 80% of its total land. Particularly, ME, NH, and VT are among the top four most heavily forested states in the United States. Mean annual temperature ranges from 10 °C in southern CT to 3 °C in the northern highlands of VT, NH, and ME. Mean annual precipitation ranges from 790 to 2550 mm, with more rainfall at higher elevations.

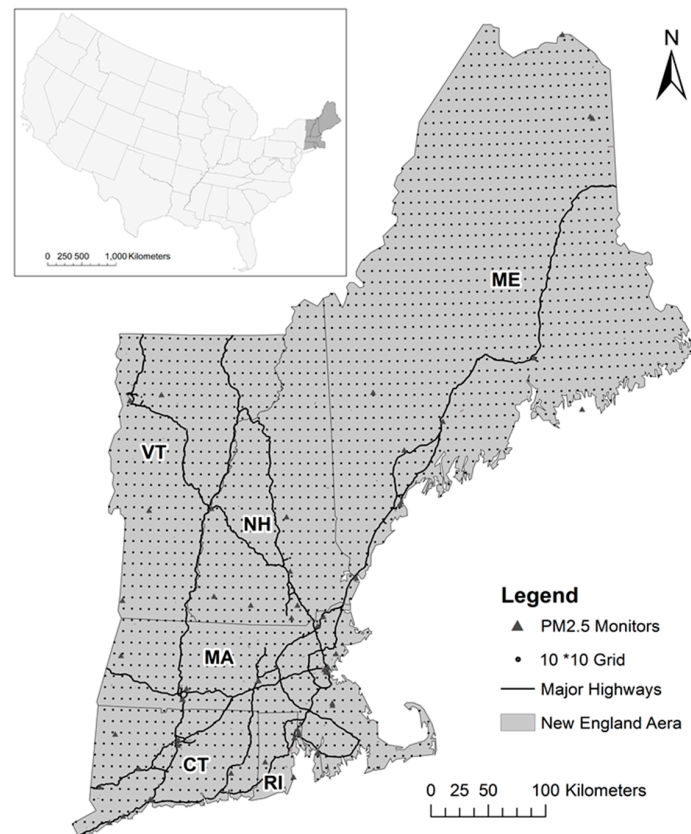


Figure 1. Map of the study area (The islands of Martha’s Vineyard, MA and town of Nantucket, MA are not shown here). The grid cell shown in the map is of 10 km × 10 km resolution.

2.2. Data

2.2.1. Ground Measurements

The ground-level PM_{2.5} measurements over New England from 1 January 2013 to 31 December 2013 were acquired from the US Environmental Protection Agency (EPA)’s Air Quality System [35]. According to Hu, Waller, Al-Hamdan, Crosson, Estes Jr, Estes, Quattrochi, Sarnatand, and Liu [20], PM_{2.5} values that fall below the detection limit were removed (<2 μg/m³). As a result, 55 monitoring sites were counted for the analysis (Figure 1). Please note that the northern area (mainly ME, NH, and VT, with very low population density and high forest coverage) has fewer PM_{2.5} monitors than the southern area (mainly CT, eastern MA, and RI, with some large cities and most urban areas).

The meteorological data were derived from two assimilated datasets. The wind speed (WS, m/s) data was obtained from the Phase 2 North America Land Data Assimilation System (NLDAS-2) [36] with a high spatial resolution (1/8th degree, or ~13 km). Since NLDAS-2 does not provide the planetary boundary layer height (PBLH, m) data, our PBLH data was obtained from the North American Regional Reanalysis (NARR) (<http://www.emc.ncep.noaa.gov/mmb/rrean/>) dataset, which has a spatial resolution of ~32 km. To be consistent with the satellite overpass time (10:30 a.m. local time for Terra, and 1:30 p.m. local time for Aqua), the mean values of the two variables were calculated for the daily time period from 9 a.m. to 3 p.m. local time.

2.2.2. Satellite Observations

The 2013 MODIS AOD Level 2 product (Collection 5.1) within the study domain was downloaded from a NASA Archive and Distribution System [37]. The AOD data consists of both retrievals from the two satellites, Terra and Aqua. The relatively fine spatial (10 km at nadir) and temporal (1–2 days)

resolution of these measurements makes them suitable for characterizing daily $PM_{2.5}$ concentration at a regional scale. High quality retrievals with Quality Assurance labels 3 were used to avoid introducing potential errors [38].

The annual cloud-free composited NTL data was obtained from a Version 4 F18 sensor (2010–2013) for the year 2013 [39]. This stable light product is the result of discarding visible band values with ephemeral events and replacing background noise with the value of 0. Consequently, the data, recorded as a digital number (DN), ranges from 1 to 63. With a scanning swath of 3000 km, the current stable light product can provide global imagery from 1992 to 2013, with a spatial resolution of 30 arc-seconds (~ 1 km).

The 2013 MODIS normalized difference vegetation index (NDVI) Level 3 product was acquired from National Aeronautics and Space Administration (NASA)'s Earth Observations (NEO) [40]. Specifically, the Terra satellite observations (MOD13A2), with a spatial resolution of 1 km and a revisit period of 16 days, were used. A detailed description of the MODIS NDVI products can be found elsewhere [41].

2.3. Methods

The predictions of $PM_{2.5}$ concentration over New England were carried out by incorporating the ground-based $PM_{2.5}$ measurement dataset and several satellite observation datasets (MODIS, VANUI, and meteorological data) into three specific GWR models with different predictor sets. The results from the proven optimal GWR model were used as the final $PM_{2.5}$ prediction. The detailed processing steps are illustrated in Figure 2.

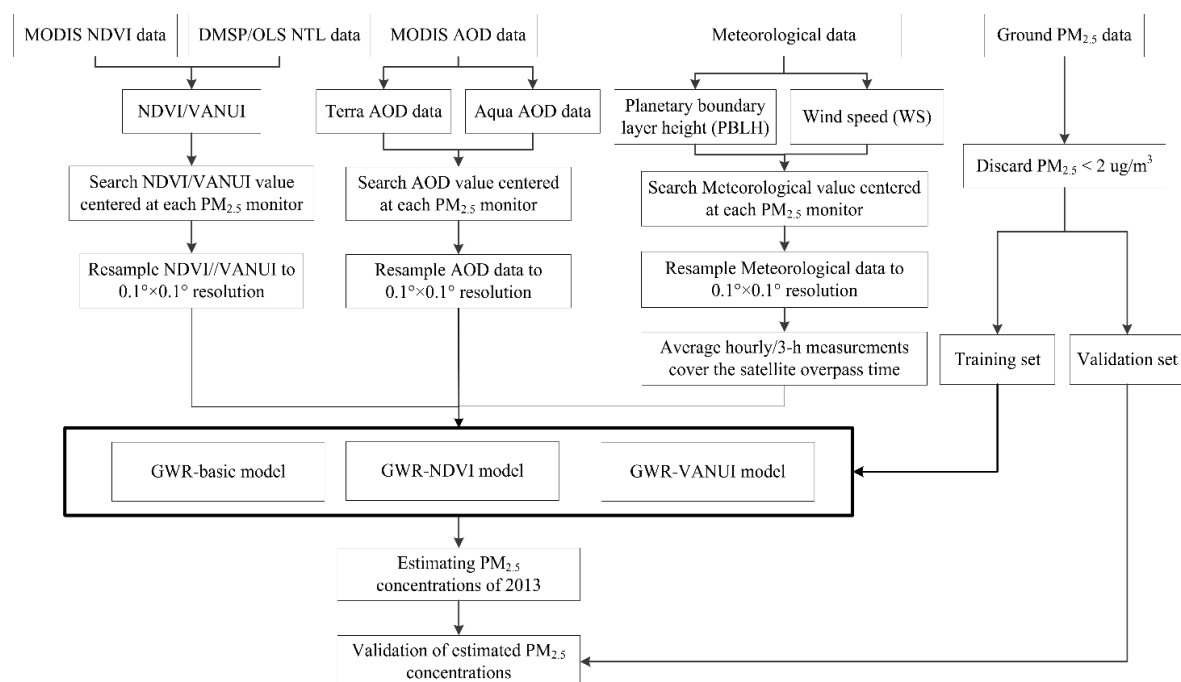


Figure 2. Flowchart outlining the $PM_{2.5}$ estimation procedures in this study. The highlighted box indicates the three different scenarios for constructing the prediction model with geographically weighted regression (GWR). With other variables (e.g., aerosol optical depth (AOD) and meteorological parameters) being the same, the main difference of the three specific GWR models lies in the incorporation of land use information: (1) GWR model without normalized difference vegetation index (NDVI) and nighttime light (NTL) data (termed as GWR-basic), (2) GWR model with NDVI data (GWR-NDVI), and (3) GWR model with vegetation adjusted NTL urban index (VANUI) data (including NDVI and NTL) (GWR-VANUI).

2.3.1. Data Pre-Processing and Integration

Before inputting the data of the dependent and independent variables into a GWR model, a uniform data resolution and map projection should be considered. A reprojection was performed to all of the datasets. Then, grid cells with 10 km resolution were built across the New England region. The data of dependent and independent variables were assigned to the nearest grid cells. The distribution of PM_{2.5} monitoring sites is uneven across the study domain, with more sites clustering in major cities like Boston. For grid cells that contain more than one PM_{2.5} monitoring site, the mean values of these sites were calculated. Similarly, the averaged AOD values were used for grid cells that contain more than one AOD observation. However, for those grid cells that have only one AOD observation available, an adjustment ratio was applied [42]. The final datasets used in this study are the products derived by spatially matching all the original data to the grid cells.

2.3.2. Model Construction

The relationships between PM_{2.5} and the predictors vary over space. Such spatial variations have been observed in previous studies [16,43–45]. Since the predictors used in our study differ from those previous studies, a comparison between the traditional multiple linear regression (MLR) (using the ordinary least squares estimator) and GWR was first conducted. The comparison showed that GWR outperformed the MLR with an improved mean accuracy of 0.15 in adjusted R², which means that GWR could explain more variance in PM_{2.5}. Therefore, using global estimation models to describe the relationships will produce less accurate results. The GWR method can estimate the spatial variation and non-stationarity of a continuous spatial variable [33], such as the PM_{2.5} concentration, at a regional scale. In other words, the regression coefficients in GWR modeling are location-specific instead of being constant globally. More applications of GWR can be found in recent publications [46,47]. In this study, a specific GWR model was designed for PM_{2.5} prediction. Four main impact factors, AOD, PBLH, WS, and VANUI, were used as explanatory variables to predict PM_{2.5} concentration in the GWR analysis (Table 1). The adaptive bandwidth was selected to account for the unbalanced distribution of the surface monitors. The specific GWR model for PM_{2.5} estimation with the four explanatory variables is expressed as

$$PM_{2.5} \sim AOD + PBLH + WS + VANUI \quad (1)$$

where $PM_{2.5}$ is the daily ground-level PM_{2.5} measurement ($\mu\text{g}/\text{m}^3$); AOD is the mean AOD averaged from MODIS AOD products onboard the Terra and Aqua satellites (unitless); $PBLH$ (m) and WS (m/s) are meteorological parameters (definitions in Section 2.2.1); and $VANUI$ is the Vegetation Adjusted NTL Urban Index (unitless).

Table 1. Description of the three specific GWR models for estimating the daily PM_{2.5} concentration.

GWR Model	Model Predictors *
GWR-basic	AOD, PBLH, WS
GWR-NDVI	AOD, PBLH, WS, NDVI
GWR-VANUI	AOD, PBLH, WS, VANUI

* AOD: aerosol optical depth. PBLH: planetary boundary layer height (m). WS: wind speed (m/s). NDVI: normalized difference vegetation index. VANUI: vegetation adjusted NTL urban index, which integrates NTL and NDVI.

The spectral index VANUI is based on Zhang et al. [48]. It has proven to be effective in reducing the NTL saturation [49] by the combined use of NTL and vegetation information, as expressed below by

$$VANUI = (1 - NDVI) \times NTL \quad (2)$$

where $NDVI$ is the MODIS Level 3 16-day NDVI value (unitless), and NTL is the normalized DMSP/OLS NTL value (unitless). The NDVI values are confined to (0, 1.0) to mask water bodies,

while the normalized NTL values are accomplished by dividing the original NTL values by 63. Thus, VANUI has a value range of 0–1. VANUI values near 1 indicate core urban areas with little vegetation, whereas VANUI values close to 0 imply areas with dense vegetation cover [48].

2.3.3. Model Validation

To assess the role of VANUI in $PM_{2.5}$ prediction, a GWR model without using VANUI (termed as GWR-basic, see Table 1) was constructed. Additionally, a GWR model with only NDVI data instead of VANUI (denoted as GWR-NDVI, see Table 1) was also constructed to specifically explore the contribution of DMSP/OLS NTL to $PM_{2.5}$ prediction. For the convenience of description, the recommended GWR model with VANUI data, as given in Equation (1), is referred as GWR-VANUI.

To test the performance of the three specific models, a 10-fold cross validation was conducted. That is, the matched dataset in all sites was first randomly divided into 10 folds. Nine folds were used for model training, while the remaining one fold served for model testing [20]. This process was iterated 10 times until every site was tested. During the procedure, the root mean squared error (RMSE), the mean absolute error (MAE), the relative root mean squared error (RRMSE), and the relative mean absolute error (RMAE) were employed to evaluate the reliability of the GWR model predictions.

3. Results

3.1. Descriptive Statistics

Figure 3 shows the histograms of all related variables, expressed in frequency distribution. The descriptive statistics (e.g., mean, standard deviation (SD), maximum, minimum, and median) for the variables are summarized in Table 2. The annual average $PM_{2.5}$ value in 2013 is $8.49 \mu\text{g}/\text{m}^3$, with a SD of $4.36 \mu\text{g}/\text{m}^3$. $PM_{2.5}$ concentration shows a typical lognormal distribution. AOD has an overall mean value of 0.13, with a SD of 0.12. As expected, the frequency distribution of AOD is more similar to that of the $PM_{2.5}$ concentration than to those of other variables. The correlation analysis verifies this point, with AOD having the highest Pearson's coefficient of 0.51 with $PM_{2.5}$. VANUI (0.52 ± 0.18) is close to a normal distribution, and similarly NDVI (0.45 ± 0.17) in the study region happens to exhibit a distribution similar to a normal distribution function. PBLH shows a lognormal distribution and has a broad value range, which is from 71 m to 1998 m. Surface wind speed ($3.23 \pm 1.64 \text{ m/s}$) tends to be a skewed normal distribution.

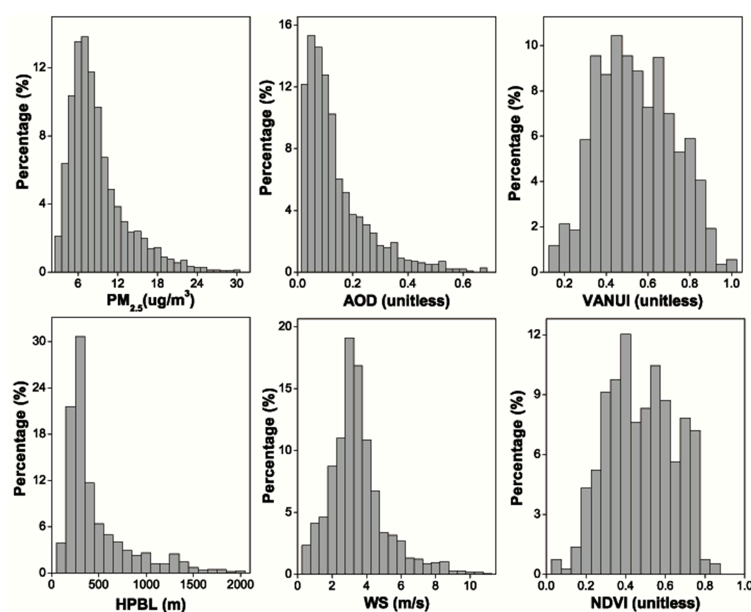


Figure 3. Histograms of all related variables used in the study.

Table 2. Descriptive statistics for all related variables.

	Mean	Std. Dev.	Min	Max	Median
PM _{2.5} (µg/m ³)	8.49	4.36	2.1	29.79	7.36
Aerosol optical depth	0.13	0.12	0.001	0.67	0.09
Vegetation adjusted NTL urban index	0.52	0.18	0.14	0.98	0.50
Normalized difference vegetation index	0.45	0.17	0.01	0.83	0.45
Planetary boundary layer height (m)	420.17	357.01	71.12	1997.97	270.32
Wind speed (m/s)	3.23	1.64	0.018	10.53	3.00

The seasonal changes for these variables is also analyzed and presented in Table 3. The mean PM_{2.5} concentrations during the winter ($9.59 \pm 5.62 \mu\text{g}/\text{m}^3$) and the summer ($10.12 \pm 5.05 \mu\text{g}/\text{m}^3$) are about 30% higher than those during the spring ($7.56 \pm 3.48 \mu\text{g}/\text{m}^3$) and the fall ($7.75 \pm 3.80 \mu\text{g}/\text{m}^3$). The mean AOD values are much higher in the spring (0.13 ± 0.10) and the summer (0.18 ± 0.14) than in the fall (0.07 ± 0.05) and the winter (0.07 ± 0.04). The highest mean value of VANUI is in the wintertime (0.68 ± 0.15) while the lowest mean VANUI value is in the summertime (0.44 ± 0.16). This may be partly due to the reduced vegetation cover as shown by NDVI (its mean value in winter decreases about 50% compared with that in summer), which results in relatively high values of VANUI according to Equation (2). The highest mean value of PBLH with the largest SD is observed in the summer ($694.85 \pm 525.03 \text{ m}$), which can be explained by strong solar radiation in the summer. On the contrary, the highest mean wind speed value is found in winter ($4.94 \pm 2.28 \text{ m/s}$).

Table 3. Seasonal summary statistics for all related variables.

Spring (N = 543)	Mean	Std. Dev.	Min	Max	Median
PM _{2.5} (µg/m ³)	7.56	3.48	2.15	24.96	6.70
Aerosol optical depth	0.13	0.10	0.001	0.57	0.09
Vegetation adjusted NTL urban index	0.55	0.17	0.15	0.88	0.55
Normalized difference vegetation index	0.42	0.15	0.11	0.76	0.41
Planetary boundary layer height (m)	469.13	424.40	72.13	1997.97	285.18
Wind speed (m/s)	3.17	1.86	0.018	10.53	2.89
Summer (N = 467)	Mean	Std. Dev.	Min	Max	Median
PM _{2.5} (µg/m ³)	10.12	5.05	2.5	29.79	9.25
Aerosol optical depth	0.18	0.14	0.001	0.67	0.15
Vegetation adjusted NTL urban index	0.44	0.16	0.14	0.96	0.41
Normalized difference vegetation index	0.54	0.16	0.03	0.83	0.54
Planetary boundary layer height (m)	694.85	525.03	105.47	1417.28	727.27
Wind speed (m/s)	2.89	1.05	0.40	6.68	2.83
Fall (N = 427)	Mean	Std. Dev.	Min	Max	Median
PM _{2.5} (µg/m ³)	7.75	3.80	2.1	25.10	7.04
Aerosol optical depth	0.07	0.05	0.001	0.36	0.06
Vegetation adjusted NTL urban index	0.55	0.19	0.14	0.98	0.54
Normalized difference vegetation index	0.41	0.17	0.01	0.74	0.38
Planetary boundary layer height (m)	465.74	373.10	71.12	1583.02	273.92
Wind speed (m/s)	3.61	1.73	0.18	10.14	3.24
Winter (N = 180)	Mean	Std. Dev.	Min	Max	Median
PM _{2.5} (µg/m ³)	9.59	5.62	3.21	20.20	6.75
Aerosol optical depth	0.07	0.04	0.023	0.20	0.08
Vegetation adjusted NTL urban index	0.68	0.15	0.46	0.98	0.70
Normalized difference vegetation index	0.27	0.13	0.01	0.50	0.26
Planetary boundary layer height (m)	310.99	173.94	72.51	1016.89	256.89
Wind speed (m/s)	4.94	2.28	2.19	8.53	3.74

Due to the shortage of the matched data records in the winter, the data was analyzed for two seasonal periods, a warm season (15 April–14 October) and a cold season (15 October–14 April), similar to that done in Lee, Liu, Coull, Schwartz, and Koutrakis [42]. The mean values of $PM_{2.5}$ for the two seasonal analysis groups are close ($8.73 \pm 4.48 \mu\text{g}/\text{m}^3$ for the warm season, and $7.73 \pm 3.89 \mu\text{g}/\text{m}^3$ for the cold season). By contrast, the mean value of AOD is much lower in the cold season (0.08 ± 0.06) than in the warm season (0.14 ± 0.12). Regional changes in rainfall and other weather parameters which increase or decrease the $PM_{2.5}$ levels might be negatively affected by this choice but in the absence of more extensive valid winter data it was the best available option.

To avoid the potential problem of strong multicollinearity among the predictor variables, Pearson's correlation coefficients were examined. The results show that the linear correlation coefficients between the predictors in individual GWR models are relatively low (Table 4). Thus, these predictors are suitable to be used together in GWR analysis. In fact, Fotheringham and Oshan [50] recently tested the sensitivity of GWR to multicollinearity and they found that GWR is very robust to the effects of multicollinearity.

Table 4. Pearson's correlation coefficient calculated among predictor variables.

	VANUI	NDVI	HPBL	WS
AOD	0.025	0.034	−0.197	−0.135
VANUI		−0.879 *	0.105	0.074
NDVI			−0.180	−0.117
HPBL				0.295

* Note that VANUI and NDVI are strongly negatively correlated, but they were not used in the same GWR model.

3.2. Model Validation

Table 5 shows the results of cross validation for the GWR-basic, GWR-NDVI, and GWR-VANUI. According to the error data (represented by RMSE, MAE, RRMSE, and RMAE), GWR-basic performed the worst. In addition, the models performed relatively better for the warm season than for the cold season, which is consistent with the previous study of Kloog et al. [51]. Here, the GWR-basic is considered as the benchmark to evaluate the predictive capabilities of GWR-NDVI and GWR-VANUI.

By adding NDVI as a predictor to the GWR-basic model, the prediction performance of the GWR-NDVI was improved by 10.5%, 3.9%, 10.08% and 3.26% in terms of RMSE, MAE, RRMSE, and RMAE, respectively, for the warm season; and by 1.8%, 1.18%, 2.26% and 0.98% for the cold season, respectively. The results are in line with other recent studies [52–54], which all indicated that land use information such as NDVI can help to predict the $PM_{2.5}$ concentration.

The VANUI, a combination of NDVI and NTL, was incorporated into the GWR-basic model to examine whether or not NTL can further improve the prediction accuracy of the $PM_{2.5}$ concentration. Based on the cross-validation results, GWR-VANUI shows significant improvement over GWR-basic in performance for the warm season, with 17%, 8.44%, 17.65% and 8.7% decreases in RMSE, MAE, RRMSE, and RMAE, respectively; and GWR-VANUI also makes obvious improvement over GWR-NDVI in performance for the warm season, with decreases of the following percentages in RMSE: 7.26%, MAE: 4.73%, RRMSE: 8.41%, and RMAE: 5.62%. A similar trend is found in the cross-validation results for the cold season. Overall, the prediction accuracy of GWR-VANUI is much higher than those of the other two models (17% higher over GWR-basic and 7.26% higher over GWR-NDVI in terms of RMSE) for the warm season, while it is still higher than the latter (3.6% higher over GWR-basic and 1.83% higher over GWR-NDVI in terms of RMSE) for the cold season. In general, GWR-VANUI performs better than GWR-NDVI and GWR-basic. The better prediction performance of GWR-VANUI indicates that the NTL data is helpful for more accurately predicting the $PM_{2.5}$ concentration.

Table 5. Ten-fold cross validation results for GWR-basic, GWR-NDVI, and GWR-VANUI.

Season	Error Index	GWR-Basic		GWR-NDVI		GWR-VANUI	
		Value	Value	Improvement (%) over GWR-Basic	Value	Improvement (%) over GWR-Basic	Improvement (%) over GWR-NDVI
Warm season	RMSE	2	1.79	10.5	1.66	17	7.26
	MAE	1.54	1.48	3.9	1.41	8.44	4.73
	RRMSE (%)	11.9	10.7	10.08	9.8	17.65	8.41
	RMAE (%)	9.2	8.9	3.26	8.4	8.7	5.62
Cold season	RMSE	2.22	2.18	1.8	2.14	3.6	1.83
	MAE	1.7	1.68	1.18	1.65	2.94	1.79
	RRMSE (%)	13.3	13	2.26	12.8	3.76	1.54
	RMAE (%)	10.2	10.1	0.98	9.8	3.92	2.97

3.3. Spatiotemporal Estimation of the PM_{2.5} Concentration

Figure 4 shows the spatial variability of PM_{2.5} in the warm season and cold season of 2013, estimated using the GWR-VANUI model. The predicted mean values of PM_{2.5} for the warm season range from 5.11 to 12.8 µg/m³, while the predicted mean values of PM_{2.5} for the cold season range from 3.69 to 8.85 µg/m³, much lower than that for the warm season. From the two maps, it can be seen that the high predicted mean values of PM_{2.5} concentration are distributed in the whole south part of New England, including CT, RI, and MA, in the warm season; however, high predicted mean values only appear in isolation in the areas of medium to large cities, such as Boston, Springfield, and Hartford, in the cold season. One possible explanation for the high level of PM_{2.5} in the warm season might be that the intense solar radiation, high temperature, and ample water vapor during summertime accelerate the formation of secondary particles [55].

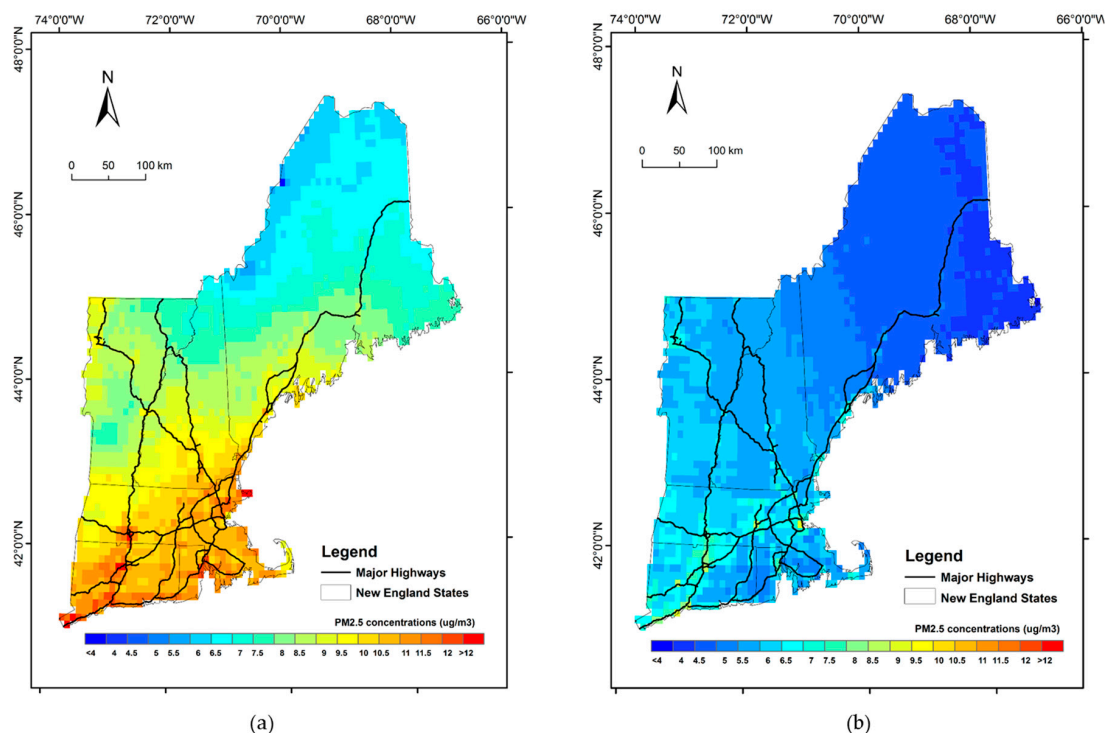


Figure 4. Spatial distribution maps of mean values of PM_{2.5} in the warm season (a) and the cold season (b) of 2013, estimated using the GWR-VANUI model.

The predicted annual mean values of PM_{2.5} in 2013 are shown in Figure 5a. The predicted values generally range from 4.7 µg/m³ near the ME border to 10 µg/m³ in New Haven, CT. By analyzing

the change trend of the annual mean values of $PM_{2.5}$ derived from all monitoring stations across New England during the period from 2000 to 2014, we find that the annual mean value decrease of $PM_{2.5}$ during 2013–2014 (10.83%) is much larger than that during 2012–2013 (5.65%), and the general decreasing trend is relatively obvious during the entire period. This might be related to the tightening of emission controls in $PM_{2.5}$. According to the newly revised National Ambient Air Quality Standards (NAAQS) issued in earlier 2013, the standard for annual $PM_{2.5}$ was set to $12 \mu\text{g}/\text{m}^3$ instead of $15 \mu\text{g}/\text{m}^3$ [56].

Despite the fact that four New England states are ranked among the top ten healthiest states in the US [57], polluted air is found in southern New England but the pollution is still below the annual standard. Compared to heavily forested and rural areas in northern New England (e.g., VT and ME), highly urbanized and populous areas in southern New England, such as Boston, Springfield, Hartford, New Haven, Bridgeport, Stamford, and Providence appear to have higher levels of $PM_{2.5}$. In addition, high $PM_{2.5}$ values are more likely to appear along highways with heavy traffic and large cities (e.g., sections of I-91 and I-95 highways in southern New England), which are essentially high emission sources. The results match well with the fact that VANUI correlates with population density and energy consumption, indicating an evident association between the $PM_{2.5}$ concentration and NTL data. It is interesting to see that within the urban areas of major cities in southern New England, the annual mean $PM_{2.5}$ concentrations are obviously high as compared to their surrounding rural forest areas, but their spatial variations tend to be low. This might be because of the regional impacts of the transported $PM_{2.5}$ pollution on these cities, as reported by a previous study [23].

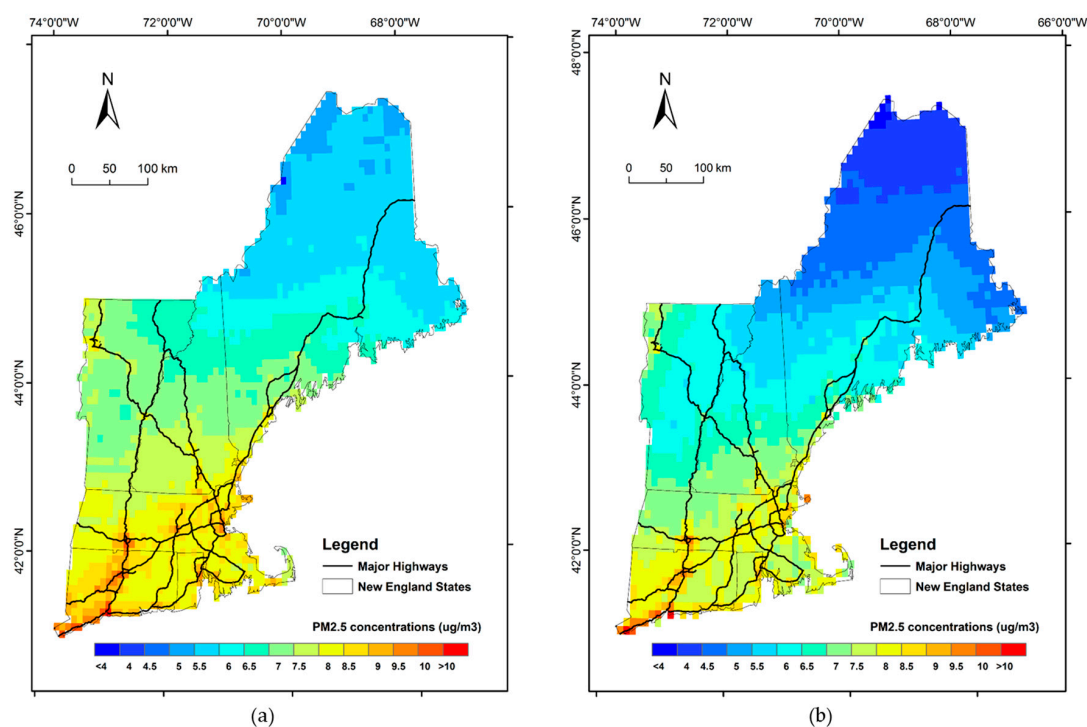


Figure 5. Spatial distribution maps of the GWR-VANUI predicted annual mean values of $PM_{2.5}$ concentration in 2013 (a) and the publicly available annual mean $PM_{2.5}$ product in 2013 (b) (downloaded from the website http://fizz.phys.dal.ca/~atmos/martin/?page_id=140).

4. Discussion

4.1. Comparison with an Available Product

To demonstrate the performance of the GWR-VANUI model, our results were also compared with one publicly available $PM_{2.5}$ product, which can be downloaded from the Dalhousie University

Atmospheric Composition Analysis Group Web site (http://fizz.phys.dal.ca/~atmos/martin/?page_id=140). This globally estimated annual mean PM_{2.5} product was based on the study of van Donkelaar et al. [58], which was produced by combining satellite-retrieved AOD with a chemical transport model and then adjusting the estimates to ground-level PM_{2.5} using GWR. To be identical to the legend of Figure 5a, the available product for 2013 with a spatial resolution of 0.1° × 0.1° was resized and replotted as shown in Figure 5b. In general, the GWR-VANUI estimated PM_{2.5} concentration map exhibits a spatial pattern similar to that of the publicly available product, but provides more details, especially in southern New England. Considering that these specific details may not be very clear on the map, a Pearson's correlation analysis was conducted between the estimated values of PM_{2.5} and the observed values. The results show that the correlation coefficient r based on the Dalhousie University product is 0.11 lower than the Pearson's correlation coefficient for the GWR-VANUI model results. The similarity in the results combined with the improved correlation and error parameters supports the hypothesis that the GWR-VANUI model results are reasonable and improve on the currently available alternative products.

Furthermore, the role of environmental background in estimating PM_{2.5} concentration was also examined. The entire New England was divided into two sub-regions: northern New England, which includes CT, MA and RI; and southern New England, which includes ME, NH and VT. The primary difference between these two sub-regions is that southern New England is more urbanized with a high population density and a low forest density, whereas northern New England is less urbanized with a low population density and a high forest density. With respect to the Pearson's correlation gradient from south to north, the r value reduces 20.5% from 0.73 to 0.58 for the predicted data of the GWR-VANUI model, and in contrast, it drops 25.8% from 0.62 to 0.46 for the available product. Overall, our study shows that the incorporation of VANUI into GWR as a predictor variable can generate more promising results, especially for urbanized and populous areas, compared with the Dalhousie University product. The spatiotemporally resolved annual PM_{2.5} estimates generated from the GWR-VANUI model could provide valuable information for epidemiological studies such as chronic effects of air pollution at regional scales [59]. In addition, health risks of exposure to PM_{2.5} could also be assessed based on the annual spatial distribution maps of PM_{2.5} concentrations produced by our model, which could serve as strong support and rationales for the effective control of PM_{2.5} emissions as well as for the practical enactment of PM_{2.5} regulations [60].

4.2. Effect of NTL

In this study, three GWR models were constructed for predicting surface PM_{2.5} concentration across New England. The model prediction results indicate that DMSP/OLS NTL data combined with NDVI data (i.e., the VANUI) can be effective for more accurately estimating PM_{2.5} concentration, especially for core urban areas. To further investigate the impact of VANUI on PM_{2.5} concentration prediction, a data sequence comparison of annual mean values of PM_{2.5}, VANUI, NTL, and NDVI at PM_{2.5} monitoring sites was conducted (Figure 6). Compared with NDVI and NTL data sequences visually, the general trend of VANUI is more similar to that of the PM_{2.5} concentration. In particular, VANUI exhibits high variability in Boston (0.70–0.59–0.67, with Site IDs of 250250002, 250250042, and 250250044, respectively). A detailed description of these monitor IDs can be found at [61]), matching well with the PM_{2.5} concentration values (7.96 µg/m³–7.35 µg/m³–7.82 µg/m³) at the same locations. However, there is not much change in the NDVI values (0.30–0.30–0.30). Conversely, in some rural areas such as New Hampshire, NDVI (0.74–0.49–0.49, with Site IDs of 330115001, 330131006, and 330150014, respectively) correlates better with the PM_{2.5} concentration values (6.25 µg/m³–7.09 µg/m³–7.10 µg/m³) than with the VANUI values (0.03–0.41–0.49). This is partly due to the fact reported in a previous study that VANUI is better at characterizing core urban variability, though it may not capture details well for cities where there is little variation in vegetation [48]. In addition, the use of VANUI successfully reduces the saturation issue confronted by NTL. For example, in core urban areas such as New Haven (Site IDs: 90090027 and 90091123), Boston

(Site IDs: 250250002, 250250042, and 250250044), Springfield (Site IDs: 250130016 and 250132009), and Providence (Site IDs: 440070022), the normalized values of NTL have already been saturated to 1. However, the VANUI values within these regions show significant variability and the variations within these intra-urban monitors can be detectable. Pearson's correlation coefficients between annual $PM_{2.5}$ concentration and the three independent variables were also calculated to assess the prediction ability of VANUI. They are 0.70 for $PM_{2.5}$ and VANUI, -0.59 for $PM_{2.5}$ and NDVI, and 0.63 for $PM_{2.5}$ and NTL, respectively. This further ascertains that DMSP/OLS NTL in combination with NDVI (i.e., the VANUI index) could be a better alternative to NDVI for more accurately estimating the $PM_{2.5}$ concentration.

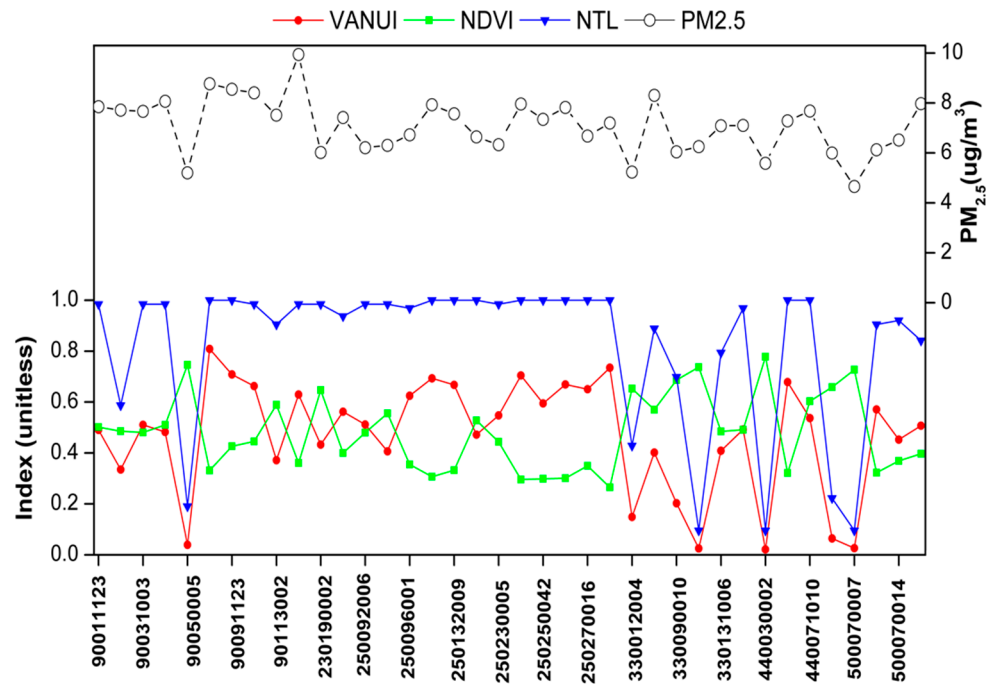


Figure 6. Data sequence comparison of annual means values of $PM_{2.5}$, Vegetation Adjust NTL Urban Index (VANUI), nighttime light (NTL), and Normalized Difference Vegetation Index (NDVI) at $PM_{2.5}$ monitoring sites located in New England.

5. Conclusions

In this paper, a pilot study was undertaken to evaluate the potential of using DMSP/OLS NTL data for $PM_{2.5}$ prediction. The case study focuses on the New England region, where both urban and rural settings are present. VANUI (an integrated index of NTL and NDVI), satellite-derived AOD measurement, and two meteorological factors were employed as predictor variables in GWR analysis for the estimation of the $PM_{2.5}$ concentration at a regional scale. We compared the specific GWR model with VANUI (i.e., GWR-VANUI) to two other specific GWR models (GWR-basic and GWR-NDVI, both of which do not use NTL). The comparison results demonstrate that the GWR-VANUI can explain more information than the two GWR models without using NTL data. We found that including NTL data can significantly improve the performance of GWR for the warm season (GWR-VANUI performed 17% better than GWR-basic and 7.26% better than GWR-NDVI in terms of RMSE), while its improvements are less obvious for the cold season (GWR-VANUI performed 3.6% better than GWR-basic and 1.83% better than GWR-NDVI in terms of RMSE). This work suggests that using NTL combined with NDVI is helpful in assessing ground-based $PM_{2.5}$ concentration.

Likewise, the spatial distribution of the predicted $PM_{2.5}$ concentration indicates the value of using DMSP/OLS NTL data for air quality monitoring. Higher concentrations of $PM_{2.5}$ expectedly occur in urbanized and populated areas and along interstate highways, while lower levels of $PM_{2.5}$ appear in

less urbanized or densely forested areas. Furthermore, the comparison of data sequences of annual mean values of PM_{2.5} and three related variables at monitoring sites shows that the integrated use of NTL and NDVI data (as the VANUI index) is a better choice for predicting PM_{2.5} concentration, especially in core urban areas, where more details can be found in the predicted PM_{2.5} surface map. Therefore, it can be concluded that the DMSP/OLS NTL imagery can be used as a valuable dataset for more accurately predicting regional PM_{2.5} pollution, and this study provides supportive evidence useful for its future application in air quality monitoring.

There are still several aspects that need further improvement in future work. One is the relatively coarse spatial resolution of the satellite-retrieved AOD product used in the study. Another issue is that the capability of current VANUI is limited by the 6-bit radiometric scale of NTL [48]. With the newly released Visible Infrared Imaging Radiometer Suite (VIIRS) onboard the Suomi National Polar-orbiting Partnership (S-NPP) spacecraft, which has a spatial resolution of 6 km for aerosol retrievals and a broader radiometric scale of 14-bit, it is expected for new opportunities to further reduce the prediction errors of PM_{2.5} concentration. Moreover, the sparse measurements in winter as well as other additional factors such as rainfall tend to limit the model prediction. In future research, we will attempt to incorporate other influential predictors into a mixed-effects model [62], which could generate daily PM_{2.5} predictions to minimize the bias.

Acknowledgments: We are grateful for the helpful comments and suggestions offered by the two anonymous reviewers for improving the quality of this paper. We also thank the MODIS Science Data Support Team and the Earth Observing System for processing, maintaining and distributing the MODIS data.

Author Contributions: Xueke Li and Chuanrong Zhang conceived and designed the framework of this research. Xueke Li performed the data processing and wrote the draft of the manuscript. Chuanrong Zhang and Weidong Li revised and edited the manuscript. Kai Liu gave advice for writing the paper.

Conflicts of Interest: The authors declare no conflict of interest.

References

1. Brunekreef, B.; Holgate, S.T. Air pollution and health. *Lancet* **2002**, *360*, 1233–1242. [[CrossRef](#)]
2. Kaufman, Y.J.; Tanre, D.; Boucher, O. A satellite view of aerosols in the climate system. *Nature* **2002**, *419*, 215–223. [[CrossRef](#)] [[PubMed](#)]
3. Dockery, D.W.; Pope, C.A.; Xu, X.; Spengler, J.D.; Ware, J.H.; Fay, M.E.; Ferris, B.G.J.; Speizer, F.E. An association between air pollution and mortality in six U.S. Cities. *N. Engl. J. Med.* **1993**, *329*, 1753–1759. [[CrossRef](#)] [[PubMed](#)]
4. Pope, C.A. Epidemiology of fine particulate air pollution and human health: Biologic mechanisms and who's at risk? *Environ. Health Perspect.* **2000**, *108*, 713–723. [[CrossRef](#)] [[PubMed](#)]
5. Dominici, F.; Peng, R.D.; Bell, M.L.; Pham, L.; McDermott, A.; Zeger, S.L.; Samet, J.M. Fine particulate air pollution and hospital admission for cardiovascular and respiratory diseases. *JAMA* **2006**, *295*, 1127–1134. [[CrossRef](#)] [[PubMed](#)]
6. Miller, K.A.; Siscovick, D.S.; Sheppard, L.; Shepherd, K.; Sullivan, J.H.; Anderson, G.L.; Kaufman, J.D. Long-term exposure to air pollution and incidence of cardiovascular events in women. *N. Engl. J. Med.* **2007**, *356*, 447–458. [[CrossRef](#)] [[PubMed](#)]
7. Rice, M.B.; Ljungman, P.L.; Wilker, E.H.; Gold, D.R.; Schwartz, J.D.; Koutrakis, P.; Washko, G.R.; O'Connor, G.T.; Mittleman, M.A. Short-term exposure to air pollution and lung function in the framingham heart study. *Am. J. Respir. Crit. Care Med.* **2013**, *188*, 1351–1357. [[CrossRef](#)] [[PubMed](#)]
8. Rice, M.B.; Ljungman, P.L.; Wilker, E.H.; Dorans, K.S.; Gold, D.R.; Schwartz, J.; Koutrakis, P.; Washko, G.R.; O'Connor, G.T.; Mittleman, M.A.; et al. Long-term exposure to traffic emissions and fine particulate matter and lung function decline in the framingham heart study. *Am. J. Respir. Crit. Care Med.* **2015**, *191*, 656–664. [[CrossRef](#)] [[PubMed](#)]
9. Van Donkelaar, A.; Martin, R.V.; Brauer, M.; Kahn, R.; Levy, R.; Verduzco, C.; Villeneuve, P.J. Global estimates of ambient fine particulate matter concentrations from satellite-based aerosol optical depth: Development and application. *Environ. Health Perspect.* **2010**, *118*, 847–855. [[CrossRef](#)] [[PubMed](#)]

10. Engel-Cox, J.A.; Hoff, R.M.; Haymet, A.D.J. Recommendations on the use of satellite remote-sensing data for urban air quality. *J. Air Waste Manag. Assoc.* **2004**, *54*, 1360–1371. [[CrossRef](#)] [[PubMed](#)]
11. Gupta, P.; Christopher, S.A.; Wang, J.; Gehrig, R.; Lee, Y.; Kumar, N. Satellite remote sensing of particulate matter and air quality assessment over global cities. *Atmos. Environ.* **2006**, *40*, 5880–5892. [[CrossRef](#)]
12. Hoff, R.M.; Christopher, S.A. Remote sensing of particulate pollution from space: Have we reached the promised land? *J. Air Waste Manag. Assoc.* **2009**, *59*, 645–675. [[PubMed](#)]
13. Liu, Y.; Franklin, M.; Kahn, R.; Koutrakis, P. Using aerosol optical thickness to predict ground-level PM_{2.5} concentrations in the st. Louis area: A comparison between misr and MODIS. *Remote Sens. Environ.* **2007**, *107*, 33–44. [[CrossRef](#)]
14. Liu, Y.; Paciorek, C.J.; Koutrakis, P. Estimating regional spatial and temporal variability of PM_{2.5} concentrations using satellite data, meteorology, and land use information. *Environ. Health Perspect.* **2009**, *117*, 886–892. [[CrossRef](#)] [[PubMed](#)]
15. Slater, J.F.; Dibb, J.E.; Campbell, J.W.; Moore, T.S. Physical and chemical properties of surface and column aerosols at a rural new england site during MODIS overpass. *Remote Sens. Environ.* **2004**, *92*, 173–180. [[CrossRef](#)]
16. You, W.; Zang, Z.; Pan, X.; Zhang, L.; Chen, D. Estimating PM_{2.5} in xi'an, china using aerosol optical depth: A comparison between the MODIS and misr retrieval models. *Sci. Total Environ.* **2015**, *505*, 1156–1165. [[CrossRef](#)] [[PubMed](#)]
17. Kumar, K.R.; Sivakumar, V.; Yin, Y.; Reddy, R.R.; Kang, N.; Diao, Y.; Adesina, A.J.; Yu, X. Long-term (2003–2013) climatological trends and variations in aerosol optical parameters retrieved from MODIS over three stations in south africa. *Atmos. Environ.* **2014**, *95*, 400–408. [[CrossRef](#)]
18. Remer, L.A.; Kaufman, Y.J.; Tanré, D.; Mattoo, S.; Chu, D.A.; Martins, J.V.; Li, R.R.; Ichoku, C.; Levy, R.C.; Kleidman, R.G.; et al. The MODIS aerosol algorithm, products, and validation. *J. Atmos. Sci.* **2005**, *62*, 947–973. [[CrossRef](#)]
19. Chu, D.A.; Tsai, T.-C.; Chen, J.-P.; Chang, S.-C.; Jeng, Y.-J.; Chiang, W.-L.; Lin, N.-H. Interpreting aerosol lidar profiles to better estimate surface PM_{2.5} for columnar aod measurements. *Atmos. Environ.* **2013**, *79*, 172–187. [[CrossRef](#)]
20. Hu, X.; Waller, L.A.; Al-Hamdan, M.Z.; Crosson, W.L.; Estes, M.G., Jr.; Estes, S.M.; Quattrochi, D.A.; Sarnat, J.A.; Liu, Y. Estimating ground-level PM_{2.5} concentrations in the southeastern U.S. using geographically weighted regression. *Environ. Res.* **2013**, *121*, 1–10. [[CrossRef](#)] [[PubMed](#)]
21. Kloog, I.; Nordio, F.; Coull, B.A.; Schwartz, J. Incorporating local land use regression and satellite aerosol optical depth in a hybrid model of spatiotemporal PM_{2.5} exposures in the mid-atlantic states. *Environ. Sci. Technol.* **2012**, *46*, 11913–11921. [[CrossRef](#)] [[PubMed](#)]
22. Koelemeijer, R.B.A.; Homan, C.D.; Matthijsen, J. Comparison of spatial and temporal variations of aerosol optical thickness and particulate matter over europe. *Atmos. Environ.* **2006**, *40*, 5304–5315. [[CrossRef](#)]
23. Lee, H.J.; Coull, B.A.; Bell, M.L.; Koutrakis, P. Use of satellite-based aerosol optical depth and spatial clustering to predict ambient PM_{2.5} concentrations. *Environ. Res.* **2012**, *118*, 8–15. [[CrossRef](#)] [[PubMed](#)]
24. Liu, Y.; Sarnat, J.A.; Kilaru, V.; Jacob, D.J.; Koutrakis, P. Estimating ground-level PM_{2.5} in the Eastern United States using satellite remote sensing. *Environ. Sci. Technol.* **2005**, *39*, 3269–3278. [[CrossRef](#)] [[PubMed](#)]
25. Zou, B.; Pu, Q.; Bilal, M.; Weng, Q.; Zhai, L.; Nichol, J.E. High-resolution satellite mapping of fine particulates based on geographically weighted regression. *IEEE Geosci. Remote Sens. Lett.* **2016**, *13*, 495–499. [[CrossRef](#)]
26. Elvidge, C.; Baugh, K.; Hobson, V.; Kihn, E.; Kroehl, H.; Davis, E.; Cocero, D. Satellite inventory of human settlements using nocturnal radiation emissions: A contribution for the global toolchest. *Glob. Chang. Biol.* **1997**, *3*, 387–395. [[CrossRef](#)]
27. Sutton, P.C.; Elvidge, C.; Obremski, T. Building and evaluating models to estimate ambient population density. *Photogramm. Eng. Remote Sens.* **2003**, *69*, 545–553. [[CrossRef](#)]
28. Yuyu, Z.; Steven, J.S.; Kaiguang, Z.; Marc, I.; Allison, T.; Ben, B.-L.; Ghassem, R.A.; Xuesong, Z.; Chunyang, H.; Christopher, D.E.; et al. A global map of urban extent from nightlights. *Environ. Res. Lett.* **2015**, *10*, 054011.
29. Zhou, N.; Hubacek, K.; Roberts, M. Analysis of spatial patterns of urban growth across south asia using dmsp-ols nighttime lights data. *Appl. Geogr.* **2015**, *63*, 292–303. [[CrossRef](#)]
30. Zhou, Y.; Smith, S.J.; Elvidge, C.D.; Zhao, K.; Thomson, A.; Imhoff, M. A cluster-based method to map urban area from dmsp/ols nightlights. *Remote Sens. Environ.* **2014**, *147*, 173–185. [[CrossRef](#)]

31. Li, R.; Liu, X.; Li, X. Estimation of the PM_{2.5} pollution levels in beijing based on nighttime light data from the defense meteorological satellite program-operational linescan system. *Atmosphere* **2015**, *6*, 607–622. [[CrossRef](#)]
32. Xu, Z.; Xia, X.; Liu, X.; Qian, Z. Combining dmsp/ols nighttime light with echo state network for prediction of daily PM_{2.5} average concentrations in shanghai, china. *Atmosphere* **2015**, *6*, 1507–1520. [[CrossRef](#)]
33. Fotheringham, A.S.; Brunson, C.; Charlton, M. *Geographically Weighted Regression: The Analysis of Spatially Varying Relationships*; John Wiley & Sons: New York, NY, USA, 2002.
34. Redman, C.; Foster, D.R. *Agrarian Landscapes in Transition: Comparisons of Long-Term Ecological & Cultural Change*; Oxford University Press: Oxford, UK, 2008.
35. US Environmental Protection Agency. Air Quality System Data Mart. Available online: <http://www.epa.gov/ttn/airs/aqsdatamart> (accessed on 14 June 2017).
36. The Phase 2 North America Land Data Assimilation System (NLDAS-2). Available online: <https://ldas.gsfc.nasa.gov/nldas/NLDAS2forcing.php> (accessed on 14 June 2017).
37. Atmosphere Archive and Distribution System. Available online: <http://ladsweb.nascom.nasa.gov> (accessed on 14 June 2017).
38. Remer, L.A.; Kleidman, R.G.; Levy, R.C.; Kaufman, Y.J.; Tanré, D.; Mattoo, S.; Martins, J.V.; Ichoku, C.; Koren, I.; Yu, H.; et al. Global aerosol climatology from the MODIS satellite sensors. *J. Geophys. Res. Atmos.* **2008**, *113*. [[CrossRef](#)]
39. Defense Meteorological Satellite Program (DMSP). Available online: <https://ngdc.noaa.gov/eog/dmsp.html> (accessed on 14 June 2017).
40. National Aeronautics and Space Administration (NASA)'s Earth Observations (NEO). Available online: <https://neo.sci.gsfc.nasa.gov/> (accessed on 14 June 2017).
41. Huete, A.; Didan, K.; Miura, T.; Rodriguez, E.P.; Gao, X.; Ferreira, L.G. Overview of the radiometric and biophysical performance of the MODIS vegetation indices. *Remote Sens. Environ.* **2002**, *83*, 195–213. [[CrossRef](#)]
42. Lee, H.; Liu, Y.; Coull, B.; Schwartz, J.; Koutrakis, P. A novel calibration approach of MODIS aod data to predict PM_{2.5} concentrations. *Atmos. Chem. Phys.* **2011**, *11*, 7991–8002. [[CrossRef](#)]
43. Engel-Cox, J.A.; Holloman, C.H.; Coutant, B.W.; Hoff, R.M. Qualitative and quantitative evaluation of MODIS satellite sensor data for regional and urban scale air quality. *Atmos. Environ.* **2004**, *38*, 2495–2509. [[CrossRef](#)]
44. Lin, G.; Fu, J.; Jiang, D.; Hu, W.; Dong, D.; Huang, Y.; Zhao, M. Spatio-temporal variation of PM_{2.5} concentrations and their relationship with geographic and socioeconomic factors in china. *Int. J. Environ. Res. Public Health* **2014**, *11*, 173–186. [[CrossRef](#)] [[PubMed](#)]
45. Song, W.; Jia, H.; Huang, J.; Zhang, Y. A satellite-based geographically weighted regression model for regional PM_{2.5} estimation over the pearl river delta region in china. *Remote Sens. Environ.* **2014**, *154*, 1–7. [[CrossRef](#)]
46. Wang, K.; Zhang, C.; Li, W. Predictive mapping of soil total nitrogen at a regional scale: A comparison between geographically weighted regression and cokriging. *Appl. Geogr.* **2013**, *42*, 73–85. [[CrossRef](#)]
47. Zhang, C.; Li, W.; Civco, D. Application of geographically weighted regression to fill gaps in slc-off landsat etm+ satellite imagery. *Int. J. Remote Sens.* **2014**, *35*, 7650–7672. [[CrossRef](#)]
48. Zhang, Q.; Schaaf, C.; Seto, K.C. The vegetation adjusted ntl urban index: A new approach to reduce saturation and increase variation in nighttime luminosity. *Remote Sens. Environ.* **2013**, *129*, 32–41. [[CrossRef](#)]
49. Elvidge, C.D.; Cinzano, P.; Pettit, D.R.; Arvesen, J.; Sutton, P.; Small, C.; Nemani, R.; Longcore, T.; Rich, C.; Safran, J.; et al. The nightsat mission concept. *Int. J. Remote Sens.* **2007**, *28*, 2645–2670. [[CrossRef](#)]
50. Fotheringham, A.S.; Oshan, T.M. Geographically weighted regression and multicollinearity: Dispelling the myth. *J. Geogr. Syst.* **2016**, *18*, 303–329. [[CrossRef](#)]
51. Kloog, I.; Koutrakis, P.; Coull, B.A.; Lee, H.J.; Schwartz, J. Assessing temporally and spatially resolved PM_{2.5} exposures for epidemiological studies using satellite aerosol optical depth measurements. *Atmos. Environ.* **2011**, *45*, 6267–6275. [[CrossRef](#)]
52. Di, Q.; Kloog, I.; Koutrakis, P.; Lyapustin, A.; Wang, Y.; Schwartz, J. Assessing PM_{2.5} exposures with high spatiotemporal resolution across the continental United States. *Environ. Sci. Technol.* **2016**, *50*, 4712–4721. [[CrossRef](#)] [[PubMed](#)]

53. Lee, M.; Kloog, I.; Chudnovsky, A.; Lyapustin, A.; Wang, Y.; Melly, S.; Coull, B.; Koutrakis, P.; Schwartz, J. Spatiotemporal prediction of fine particulate matter using high-resolution satellite images in the southeastern US 2003–2011. *J. Expo. Sci. Environ. Epidemiol.* **2016**, *26*, 377–384. [[CrossRef](#)] [[PubMed](#)]
54. Ma, L.; Wu, J.; Li, W.; Peng, J.; Liu, H. Evaluating saturation correction methods for dmsp/ols nighttime light data: A case study from china's cities. *Remote Sens.* **2014**, *6*, 9853–9872. [[CrossRef](#)]
55. Hu, X.; Waller, L.A.; Lyapustin, A.; Wang, Y.; Al-Hamdan, M.Z.; Crosson, W.L.; Estes, M.G., Jr.; Estes, S.M.; Quattrochi, D.A.; Puttaswamy, S.J.; et al. Estimating ground-level PM_{2.5} concentrations in the Southeastern United States using maiaac aod retrievals and a two-stage model. *Remote Sens. Environ.* **2014**, *140*, 220–232. [[CrossRef](#)]
56. Air quality: Epa's 2013 Changes to the Particulate Matter (Pm) Standard. Available online: <http://www.nationalaglawcenter.org/wp-content/uploads/assets/crs/RL33254.pdf> (accessed on 3 May 2017).
57. America's Health Rankings. Available online: <http://cdnfiles.americashealthrankings.org/SiteFiles/Reports/Americas-Health-Rankings-2012-v1.pdf> (accessed on 3 May 2017).
58. van Donkelaar, A.; Martin, R.V.; Spurr, R.J.D.; Burnett, R.T. High-resolution satellite-derived PM_{2.5} from optimal estimation and geographically weighted regression over north america. *Environ. Sci. Technol.* **2015**, *49*, 10482–10491. [[CrossRef](#)] [[PubMed](#)]
59. Kloog, I.; Coull, B.A.; Zanobetti, A.; Koutrakis, P.; Schwartz, J.D. Acute and chronic effects of particles on hospital admissions in new-england. *PLoS ONE* **2012**, *7*, e34664. [[CrossRef](#)] [[PubMed](#)]
60. Peng, J.; Chen, S.; Lü, H.; Liu, Y.; Wu, J. Spatiotemporal patterns of remotely sensed PM_{2.5} concentration in china from 1999 to 2011. *Remote Sens. Environ.* **2016**, *174*, 109–121. [[CrossRef](#)]
61. AirData Download Files Documentation. Available online: <https://aqsdrl.epa.gov/aqsweb/aqstmp/airdata/FileFormats.html> (accessed on 14 June 2017).
62. Kloog, I.; Chudnovsky, A.A.; Just, A.C.; Nordio, F.; Koutrakis, P.; Coull, B.A.; Lyapustin, A.; Wang, Y.; Schwartz, J. A new hybrid spatio-temporal model for estimating daily multi-year PM_{2.5} concentrations across northeastern USA using high resolution aerosol optical depth data. *Atmos. Environ.* **2014**, *95*, 581–590. [[CrossRef](#)]



© 2017 by the authors. Licensee MDPI, Basel, Switzerland. This article is an open access article distributed under the terms and conditions of the Creative Commons Attribution (CC BY) license (<http://creativecommons.org/licenses/by/4.0/>).